https://ntrs.nasa.gov/search.jsp?R=20070031910 2019-08-30T01:46:11+00:00Z

VIBRATION INSTITUTE 31ST ANNUAL MEETING, SAN ANTONIO TEXAS, JUNE 19-22, 2007

WHIRL MOTION OF A SEAL TEST RIG WITH SQUEEZE-FILM DAMPERS

Edgar J. Gunter
RODYN Vibration Analysis, Inc.
DrGunter@aol.com

Margaret P. Proctor
NASA Glenn Research Center
Margaret.P.Proctor@nasa.gov

ABSTRACT

This paper presents the experimental behavior and dynamic analysis of a high speed test rig with rolling element bearings mounted in squeeze film oil damper bearings. The test rotor is a double overhung configuration with rolling element ball bearings mounted in uncentered squeeze-film oil dampers. The damper design is similar to that employed with various high-speed aircraft HP gas turbines. The dynamic performance of the test rig with the originally installed dampers with an effective damper length of length 0.23-inch was unacceptable. The design speed of 40,000 RPM could not be safely achieved as nonsynchronous whirling at the overhung seal test disk and high amplitude critical speed response at the drive spline section occurred at 32,000 RPM. In addition to the self excited stability and critical speed problems, it was later seen from FFT data analysis, that a region of supersynchronous dead band whirling occurs between 10,000 to 15,000 RPM which can lead to bearing distress and wear. The system was analyzed using both linear and nonlinear techniques. The extended length damper design resulting from the analysis eliminated the rotor subsynchronous whirling, high amplitude critical speed, and the dead band whirling region allowing the system to achieve a speed of 45,000 RPM. However, nonlinear analysis shows that damper lockup could occur with high rotor unbalance at 33,000 RPM, even with the extended squeeze-film dampers. The control of damper lockup will be addressed in a future paper.

Keywords: Nonlinear whirl response, squeeze-film dampers, damper lockup, dead band whirl

INTRODUCTION

The NASA high temperature, high speed seal rig is designed to test seals over a range of conditions including conditions expected in advanced gas turbine engines. The double overhung rotor has an 8.5 inch seal test disk and is supported by rolling element bearings in squeeze film dampers. The maximum design speed of 43,140 rpm could not originally be achieved due to the occurrences of whirling at the seal test disk and high vibrations at the spline connection to the drive shaft. There were indications of both sub- and super-harmonic whirl motion at the seal test disk and high synchronous response at the balance piston and drive spline. Experimental data indicated both a critical speed and whirling problem with the rig. A nonlinear jump response region was observed between 10,000 to 15,000 RPM with superharmonic excitation. This region is referred to as dead band whirling and occurs even with a well balanced system.

The precise design of squeeze film dampers is complicated by the highly nonlinear nature of the dampers. Initial linear analysis of critical speeds and optimum damping for various assumed bearing stiffness values serve as a useful guide. The original damper was designed with the feature that the damper length could be easily extended if needed.

The critical speed analysis of the complete system including the drive train showed that the first two critical speeds are associated with the seal test rotor. Nonlinear synchronous unbalance and time transient whirl simulations were computed for the seal test rotor with the original dampers to simulate the whirling and high synchronous response observed. With the original damper design, the nonlinear synchronous response showed that unbalance could cause damper lockup at 33,000 rpm. Alford cross-coupling forces were also included at the overhung seal test disk for the whirl analysis. Subsynchronous whirling at the seal test disk was observed in the nonlinear time transient analysis. With the extended damper length of 0.50 inch, the subsynchronous motion was eliminated and the rotor unbalance response was acceptable to 45,000 rpm with moderate rotor unbalance. However, the nonlinear analysis shows that with high rotor unbalances, damper lockup could also be obtained at 33,000 rpm, even with the extended squeeze-film dampers. Therefore, the test rotor must be reasonably balanced in order for the uncentered dampers to be effective.

1. SEAL TEST ROTOR

1.1 Description of Rotor System and Instrumentation

The seal test rotor, shown in Figure 1, consists of a high temperature alloy shaft with two overhung disks. The test rotor is supported in two rolling element bearings. These bearings are in turn supported in squeeze film damper bearings.

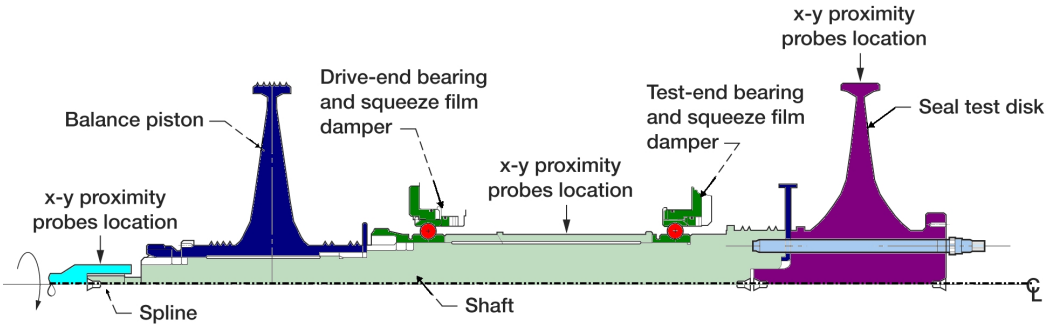

Figure 1 Seal Test Rotor Showing X-Y Proximity Probe Locations

The 8.5-inch, overhung seal test disk is piloted into the end of the shaft and clamped in place with six studs and retaining nuts. A test end insert is clamped between the seal test disk and the shaft and provides a rotor for a single knife-edge, which is part of an air buffer seal that prevents hot gases from reaching the oil-lubricated bearings. The balance piston is mounted on the opposite end of the shaft and is retained by a stainless steel lock washer and locknut. The split inner race angular contact ball bearings are mounted on the shaft between the two disks and separated by a bearing spacer. They are clamped in position by a shoulder on the shaft and a stainless steel lock washer and locknut. The bearings are mounted in oil squeeze-film dampers. The drive end of the shaft has an external spline. The drive system consists of a 60 hp air turbine and a torque meter connected to each other by a jack shaft with internal, straight splines at both ends. A similar jack shaft connects the torque meter to the seal test rotor. The alignment of the drive system to the seal test rotor is fixed by the housings for the jack shafts, torque meter and turbine, which pilot to each other and pilot to the seal test rig housing.

1.2 Instrumentation and Vibration

Proximity probes are used to observe the seal test rotor's dynamic performance. Eddy-current proximity probes at the spline and mid-span between the bearings are located at the 9 and 12 o'clock positions, when looking from the seal test disk towards the drive end, to view shaft orbits. For some tests, high-temperature capacitance proximity probes are installed at the 3, 6, 9, and 12 o'clock

positions to view the seal test disk orbit and centrifugal growth. X-Y accelerometer pairs are mounted on the seal tester housing near the drive end bearings at the 9 and 12 o'clock positions and on the air turbine at the 12 and 3 o'clock positions. These measurements along with shaft speed are recorded on a digital tape recorder. Orbits are monitored on oscilloscopes and a spectrum analyzer is used to look at the amplitude and frequency content of the signals.

1.3 Test Rig X-Y Synchronous Accel Measurements

Fig. 3 represents the seal test rig synchronous X and Y accelerometer vs speed to 34,000 RPM. An apparent vertical system resonant mode is observed at 20,000 RPM. A much stronger resonance mode for the X accelerometer observed at 32,000 RPM. The difference between the vertical and horizontal accel readings is due to the differences in bearing and support horizontal and vertical stiffness and damping values for the two planes. This asymmetry effect is often observed in uncentered dampers with moderate unbalances. Fig. 4 shows the synchronous vertical turbine accel values as rotor speed increases. Above 32,000 RPM, there is observed a rapid increase in the turbine synchronous response measurement. There was also observed fractional frequency whirl motion in the turbine orbits at higher speeds. A further increase in the seal test rotor speed to its design speed of over 40,000 RPM could have resulted in rig damage.

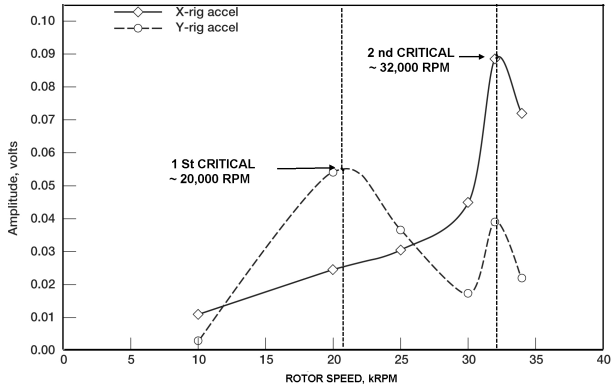

Fig. 3 X-Y Rig Synchronous Accel Vs Speed

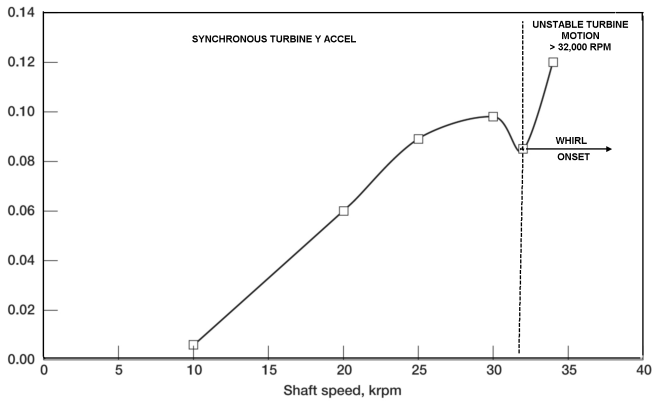

Fig 4 Turbine Y Synchronous Accel Vs Speed

1.4 Seal Test Disk Orbits

Fig. 5 represents an orbit obtained from the seal disk. Note the occurrence of the double loop. Subharmonics of ½, 1/3 and superharmonics have been observed. This could be an indication of rubbing. Fig. 6 represents a time exposure of the seal test disk motion. The orbital motion indicates impeller whirling. Above 32,000 RPM, the whirl motion increases.

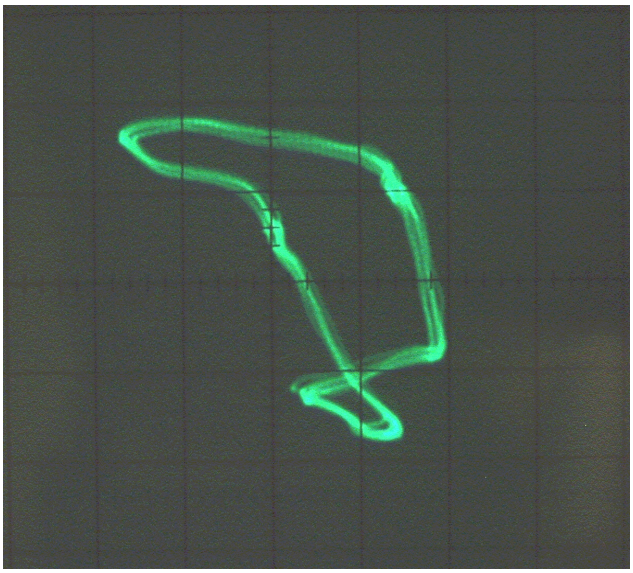

Fig. 5 Seal Test Disk Orbit With Double Loop

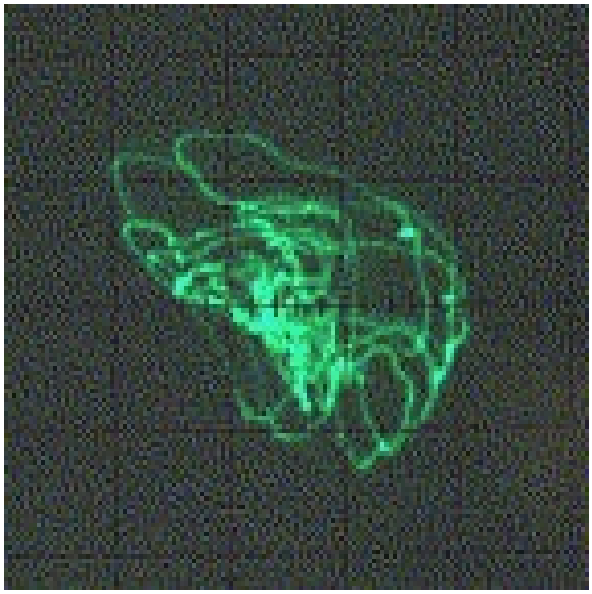

Fig. 6 Seal Test Disk Showing Whirling

1.5 Bode and Waterfall Plots Showing Dead Band Whirl Region

Fig. 7 represents the Bode plot of the synchronous motion of the test disk vertical motion. There is a jump in amplitude at 10,000 RPM which does not appear to be associated with a critical speed. The high amplitude region ends at 15,000 RPM with an abrupt jump down in amplitude. Fig. 8 represents the waterfall frequency of this spectrum. The region between 10,000 - 15,000 RPM shows the excitation of super-synchronous harmonics. In Fig. 7, it is seen that there is a 180 deg shift in phase at 20,000 RPM. This corresponds to the rotor 1st critical speed. The region between 10,000-15,000 RPM represents a region of dead band whirling of the rolling element bearings in the damper clearance spaces. Operation of the rotor in this speed range can lead to bearing distress. Fig. 8 also show that above 30,000 RPM, indications of subsynchronous whirling are encountered.

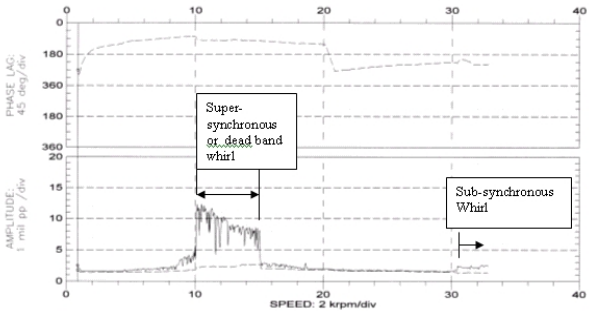

Fig. 7 Bode Plot of Test Disk Showing Dead Band Whirl Region

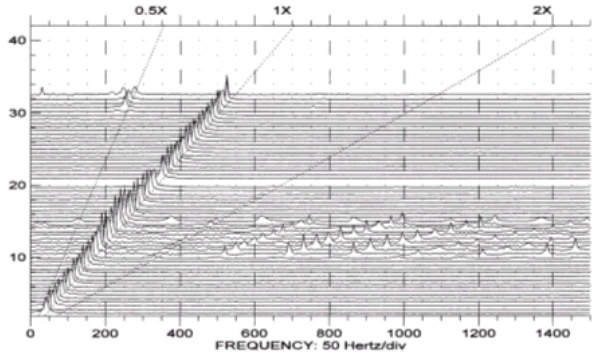

Fig. 8 Waterfall Plot of Test Disk Frequency Spectrum

2. CRITICAL SPEED ANALYSIS

2.1 Critical Speed Analysis of Test Rig

As a first step in the evaluation of the dynamical characteristics of the seal test rig, a model was generated of the entire test system including the drive turbine, torque tube and spline shafts. Since high vibrations are also encountered at the drive end spline connecting the seal test rotor, it was important to determine if the drive system could be a contributing factor. Fig. 9 represents the system first critical speed. With the nominal bearing values selected, it is seen the first system critical speed is a conical mode of the test rotor. The first critical speed in this model is 21,113 RPM. Note that the experiment rotor motion as shown in Fig. 3 indicates a resonance around 20,000 RPM. With the conical rotor motion, the bearing amplitudes are large and hence high damping should be provided in this mode. Note that the quill drive shaft isolates the test rotor from the drive system.

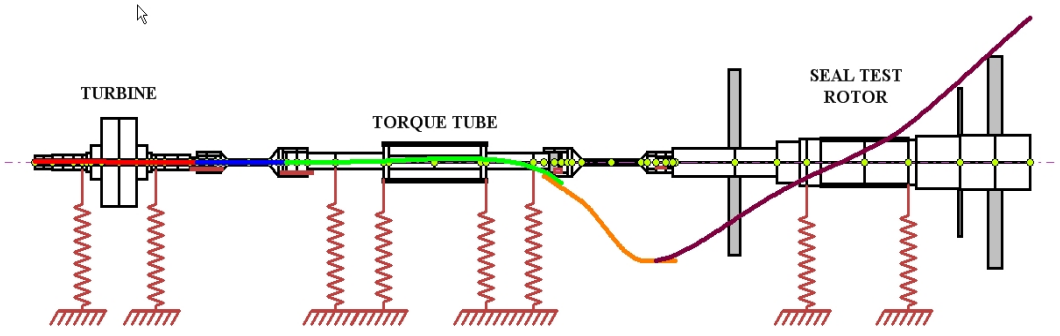

Fig. 9 Test Rig 1st Critical Speed at 21,113 RPM Showing Conical Seal Test Rotor Motion

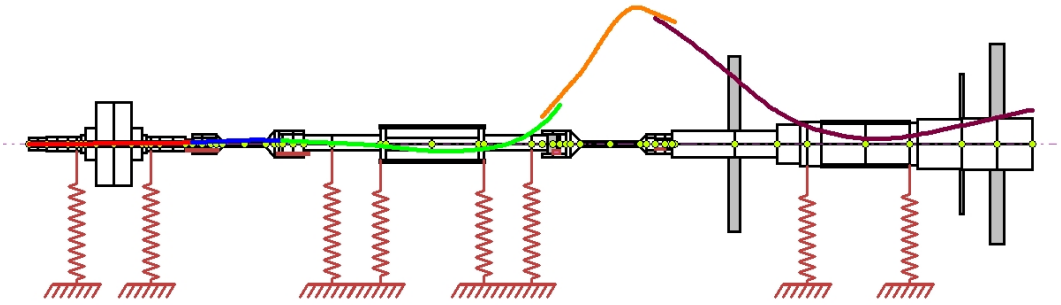

Fig. 10 Test Rig 2nd Critical Speed at 33,500 RPM RPM Showing High Drive Spline Motion-Balance Piston and Seal Impeller In Phase

Fig. 10 represents the system second critical speed mode at approximately 33,000 RPM. This high amplitude of motion at the drive spline could cause the spline to become disconnected. In the second mode, there is more strain energy in bending than in the 1st mode. The majority of the strain energy for the 1st mode is in the test rotor bearings. From an examination of the system strain and kinetic energies, it is noted that the first 2 system modes are related to the seal test rotor and the drive components may be ignored.

2.2 Critical Speed Analysis of Seal Test Rotor

Seal Test Rotor Model

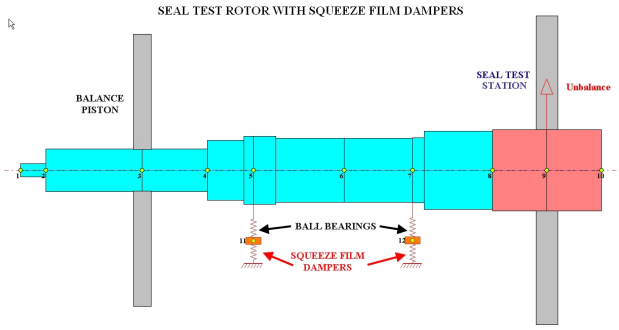

Fig. 11 Seal Test Rotor With Squeeze Film Dampers

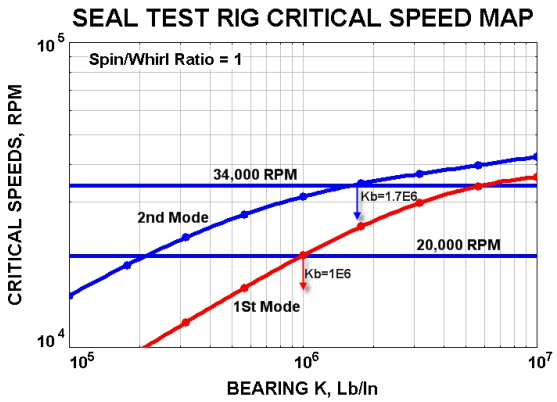

Fig. 12 Critical Speed Map

Seal Test Rotor Critical Speeds With Linear Bearings

Fig. 11 represents a model of the seal test rotor. The rotor is supported in ball bearings. The rolling element bearings are in turn supported in uncentered squeeze film dampers. The analysis of the squeeze film damper is highly nonlinear. However, it is still of value to evaluate the rotor undamped critical speeds in order to determine the rotor mode shapes and the corresponding energy distribution for each mode.

Fig. 12 represents the critical speed map for the test rotor for the first two modes as a function of bearing stiffness. On the critical speed map are drawn the speed lines for 20,000 RPM and 34,000 RPM. With a nominal bearing stiffness value of 1e6 Lb/In, the 1st critical speed is predicted to be 20,000 RPM. This corresponds to the first frequency as seen in Fig. 3. As the speed increases, the bearing stiffness increases with loading. The 2nd critical speed is predicted to be 34,000 RPM for an assumed bearing stiffness of 1.7e6 Lb/In. as shown in Fig.12.

Fig. 13 represents the rotor first critical speed mode at 20,088 RPM corresponding to an assumed total effective bearing stiffness of 1.0e6 Lb/In. Fig. 13 shows that the 1st mode is essentially a conical rigid body mode in which the seal impeller and the balance piston out of phase. For this modet, the motion is essentially rigid body conical whirling motion with the majority of the strain energy associated with the bearings. This mode shape also implies that 2 plane balancing will be sufficient to balance this mode. The subsynchronous whirling observed should be a conical mode.

At higher shaft speeds, the outboard bearing or seal test end bearing will be the principal bearing required to control subsynchronous whirling since it has a higher strain energy.

Fig. 14 represents the second critical speed at 31,291 for an assumed bearing stiffness of 1.0e6 Lb/In stiffness..

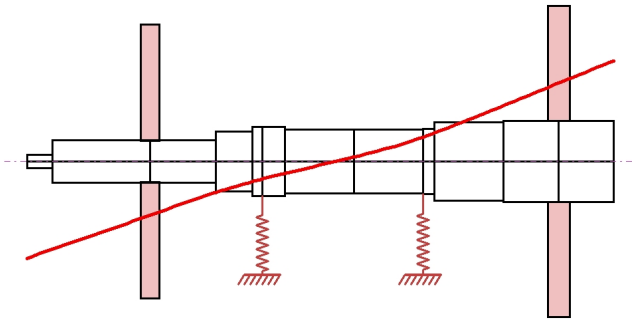

Fig. 13 1st Mode At 20,888 RPM With Kb=1e6 Lb/In

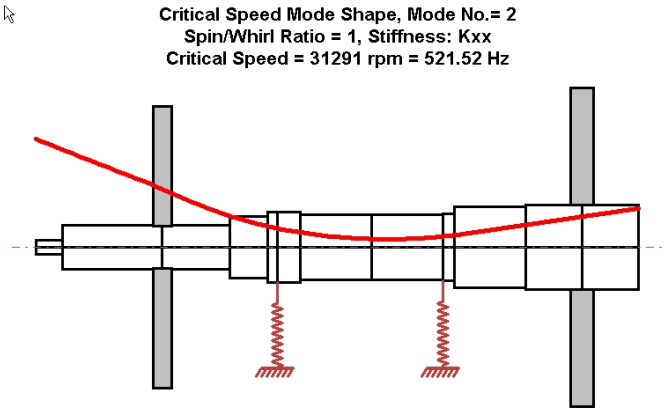

Fig. 14 2nd Mode At 31,291 RPM With Kb=1e6 Lb/In

The test end bearing has the major influence on the first critical speed. From this it can be implied that this is the principal bearing that must be modified to control subsynchronous whirl motion. In order to control the second critical speed and the high amplitude observed at the drive shaft location, the inboard bearing must be modified since the outboard bearing has a majoroty of the strain energy.

3. DYNAMIC ANALYSIS WITH ORIGINAL SQUEEZE FILM DAMPER DESIGN

3.1 Squeeze-film Dampers

The unbalance response of the seal test rig with the rolling element bearings mounted in squeeze film dampers is highly nonlinear in nature. The squeeze-film dampers are formed by the geometry of the bearing holder and the outer race of the bearing. The test end squeeze film damper, shown in Fig. 15 is formed at 2.90-inch diameter D, has a length L of 0.23 inch, and has a radial clearance C of 0.002 inch. MIL-23699 oil is supplied to the damper through 3 oil inlets.

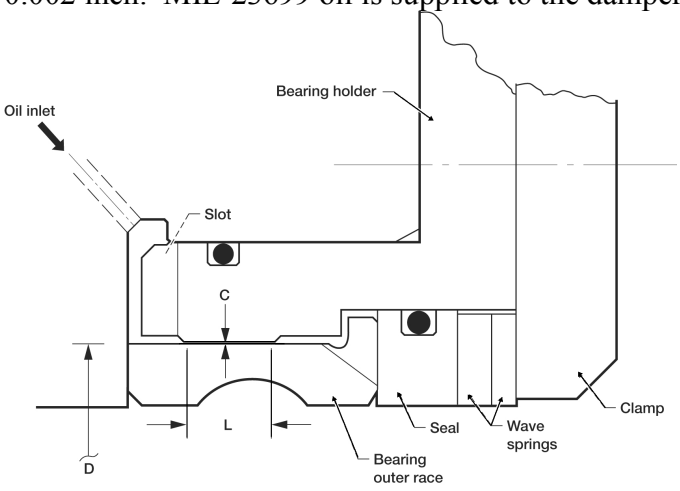

Fig. 15 Seal Impeller Damper Bearing

The slot in the left end of the bearing holder provides a route for thermocouple wires that measure the bearing outer race temperature. There is no path for the oil to exit the test end squeeze film damper. The drive-end squeeze film damper has the same dimensions and is mounted in a similar fashion, except that oil can flow through it.

The damper is referred to as an uncentered squeeze film damper since it does not have a mechanical retaining spring. The damper design is similar to that encountered in various HP aircraft gas turbine rotors. Therefore, the damper design and test results have significance towards design of damper bearings for various aircraft engine components.

Squeeze Film Synchronous Stiffness and Damping Coefficients

For the analysis of the synchronous unbalance of the test rotor, the bearing assembly is considered as a combination of the rolling element bearing in series with the uncentered squeeze film damper.

The damper motion consists of precession but not rotation. Since the damper aspect ratio L/D < 1, the short bearing pi film version of Reynolds equation may be applied. For the case of unbalance response, a further assumption is made concerning the damper motion.. It is assumed that the motion is circular synchronous precession about the bearing center. This assumption is equivalent to the assumption that the rotating load exceeds the gravitational bearing loading. Under these assumptions, the nonlinear stiffness coefficient is given as follows:

$$K_d(\varepsilon,\omega)=\frac{2\mu R\varepsilon\omega}{(1-\varepsilon^2)^2}\left(\frac{L}{C}\right)^3 \qquad (1)$$

The damper radial stiffness K_d is a function of speed and eccentricity ratio. As the damper orbits outward to larger eccentricities, then the damper stiffness increases.

At eccentricity ratios above 0.9 then the radial damper stiffness becomes quite large. The effective stiffness of the bearing assembly then approaches the combined stiffness of the rolling element bearing and the bearing support system. This condition is referred to as damper lockup and is equivalent to dead band whirl in a rolling element bearing. High bearing forces occur under these circumstances. The corresponding damping coefficient is given by

$$C_d(\varepsilon)=\frac{\pi\mu R}{2(1-\varepsilon^2)^{3/2}}\left(\frac{L}{C}\right)^3 \qquad (2)$$

Eq. 2 shows the dramatic effect of an increase of the damper length L. A doubling of damper length results in an 8 fold increase in damping for the same eccentricity ratio.

3.2 Nonlinear Synchronous Unbalance Response With Original Damper Design

An unbalance response was computed with the original length dampers of 0.23 inches and a 2 mil radial clearance. Fig 16 represents the unbalance response with the nonlinear stiffness and damping coefficients as given in Eqs. 1 and 2.

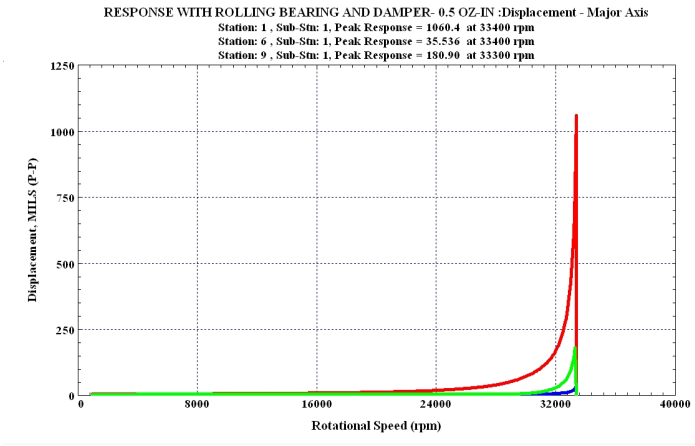

Fig. 16 Unbalance Response With Original Damper Design Showing Rotor Failure With 0.5 OZ-In

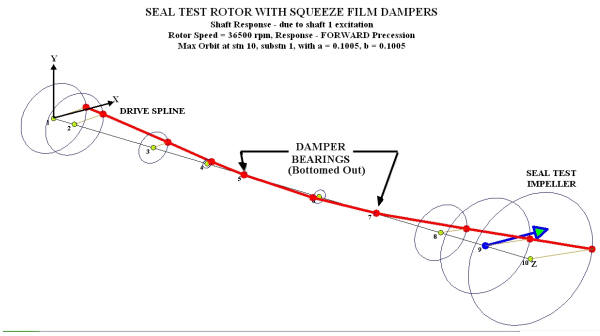

Fig. 17 Rotor Unbalance Mode Shape At 33,000 RPM Showing Damper Lockup

Fig. 16 shows that the synchronous unbalance response increases rapidly at speeds above 33,000 RPM. If the rotor speed were increased to the design speed of over 40,000 RPM, then test rotor damage could occur. Fig. 17 shows the 3 dimensional mode shape at 33,000 RPM. The unbalance is located on the seal test disk. The rotor rotating mode shape corresponds closely to the 2nd mode as shown in Fig. 13. In the unbalance response mode shape, note that the bearings are bottomed out. Since there is zero amplitude at the bearings, then there can be no contribution of damping from the bearings. Thus, when the squeeze film damper bearings bottom out or lockup, it is not possible to safely pass through the higher critical speed.

3.2 Time Transient Motion of Seal Test Rig With Original Damper Design

In the previous section on unbalance response, assumptions were made on the motion as to circular synchronous precession about the bearing origin. This shows useful information as to the high vibrations encountered at the drive spline. In order to examine the possibility of nonsynchronous or whirl motion it is necessary to perform a time transient analysis.

Fig. 18 represents the time transient analysis options of the ***DyRoBes*** rotor dynamics program for the generalized rotor dynamic motion. In this case the Newmark-Beta method of integration was selected for the numerical procedure. Other options are 4th order Runge-Kutta and the Wilson Theta method. Selected in addition to unbalance are gravitational loads as shown in Fig. 18. In the time transient analysis, the damper forces are computed at each time step based on the damper instantaneous displacement and velocity values. No bearing coefficients are employed.

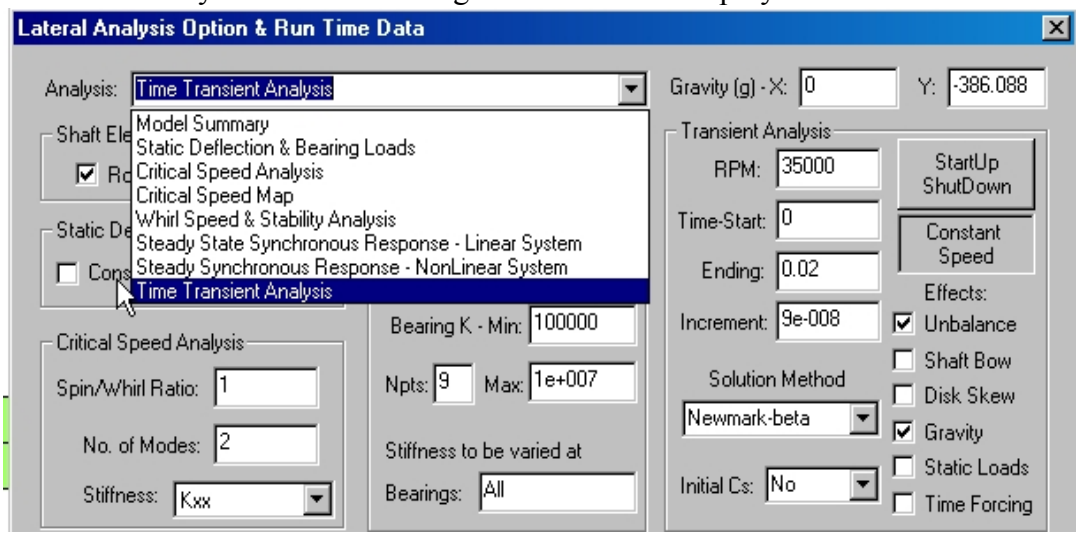

Fig. 18 Time Transient Analysis Options

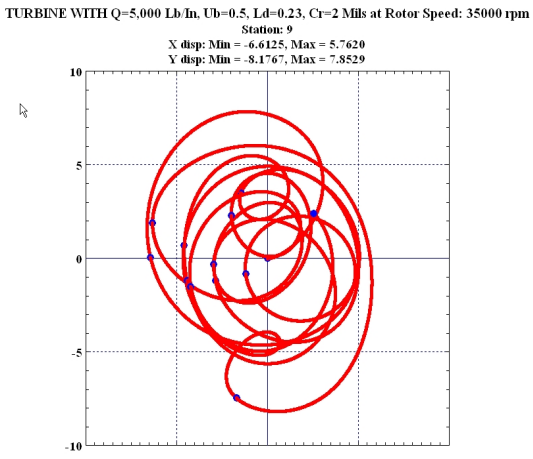

Fig. 19 Seal Impeller Orbit With Unbalance and Aero Cross Coupling Q=5,000 Lb/In at 33,000 RPM

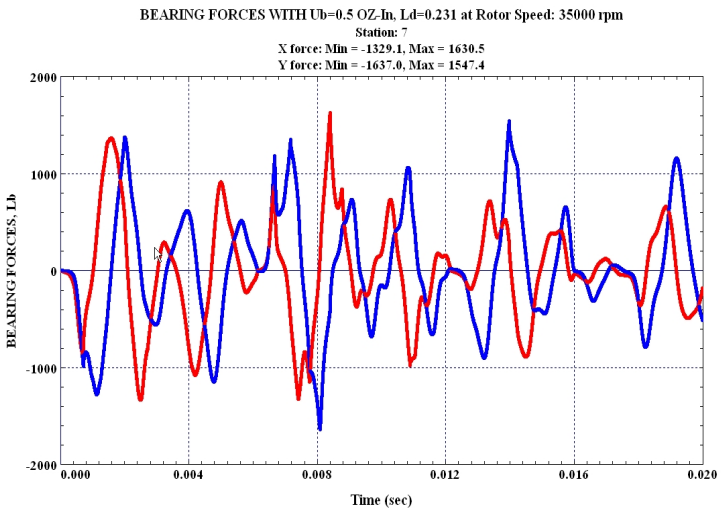

Fig. 20 Outboard Damper Bearing Transient Forces At 33,000 RPM

Fig. 19 shows the transient motion of the seal test disk with suddenly applied unbalance and an assumed value of aerodynamic cross coupling coefficient of Q=5,000 Lb/In. This Alford type effect is created by assuming a bearing station at the seal test disk and assigning Kxy =- Kyx = Q. The impeller orbit as shown in Fig. 19 indicates that the system is sensitive to small cross coupling forces that could be

generated in typical seals. Fig. 19 indicates that the maximum orbit may exceed 8 mils. This could also lead to seal rubs which can generate super as well as subharmonic frequencies.
Fig. 20 shows the transient outboard bearing forces transmitted. These bearing loads are excessive and can result in diminished rolling element bearing life. The bearing loading is similar to the loads encountered with a rolling element bearing undergoing dead band whirl with a 2 mil clearance. It is apparent from the unbalance response plot of Fig. 16 and the whirl orbit as show in Fig. 19 that the dampers are insufficient to provide adequate damping for control of seal test disk whirling or control of the high amplitude of vibration encountered at the drive spline at the 2nd critical speed.

4. DYNAMIC ANALYSIS WITH ENHANCED SQUEEZE FILM DAMPERS

4.1 Nonlinear Synchronous Unbalance Response With Enhanced Damper Design

It is apparent from the unbalance and whirl analysis of Section 3 that the squeeze film damping is inadequate. An analysis was performed with enhanced dampers with the damper length increased from 0.23 to 0.5 inches. Fig. 21 represents the unbalance response with the enhanced dampers and two planes of unbalance of 0.1 OZ-In at 90° relative phase. With improved damping and the reduced level of unbalance, the response is smooth to 50,000 RPM. Fig 22 represents the synchronous mode shape at 45,000 RPM. The rotor has little shaft bending.

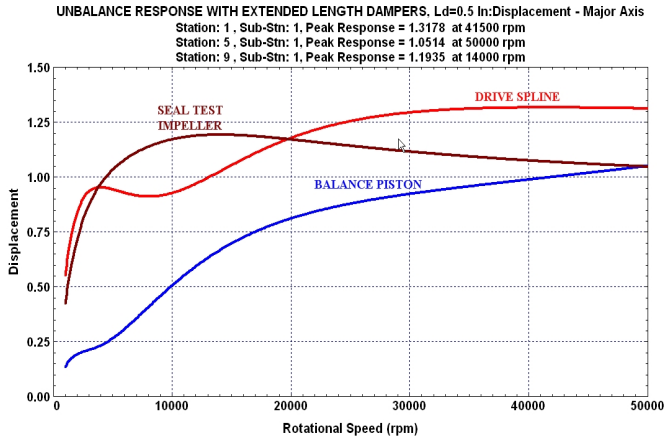

Fig. 21 Unbalance Response With Enhanced Dampers With Unbalance=0.1 OZ-In @90 at Impeller And Balance Piston

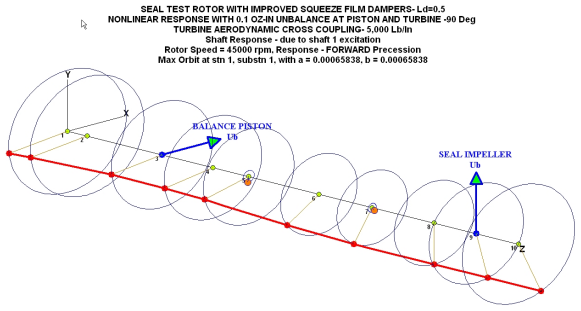

Fig. 22 Shaft Mode Shape at 45,000 RPM

4.2 Time Transient Motion of Seal Test Rig With Enhanced Damper Design

Transient Motion At 35,000 RPM With 2 Planes Ub=0.1 And Aero Cross Coupling Q

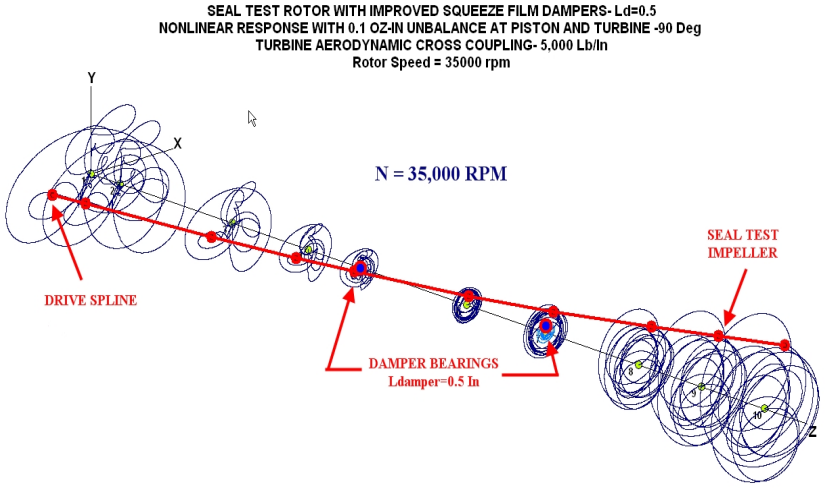

Fig. 23 Transient Rotor Motion at 35,000 RPM With Enhanced Squeeze Film Dampers, Ub=0.1

Fig. 23 shows the transient response at 35,000 RPM. Note the conical shaft motion with active damper motion. Fig. 24 represents the outboard bearing forces transmitted. The initial 1st forward conical mode rapidly damps out leaving only the synchronous unbalance response. There is no indication of self excited whirl motion present in the transient data.

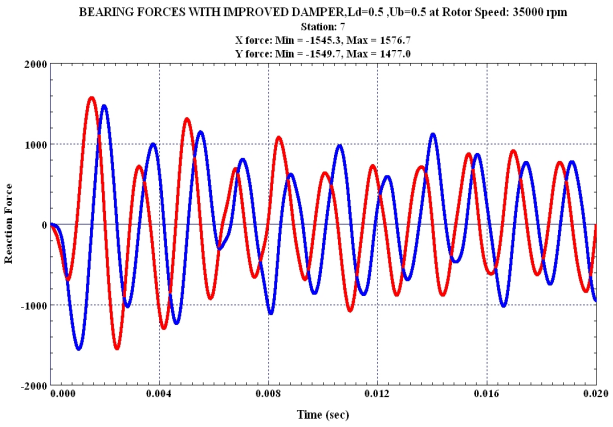

Fig. 24 Outboard Bearing Forces Transmitted

Transient Response At 45,000 RPM

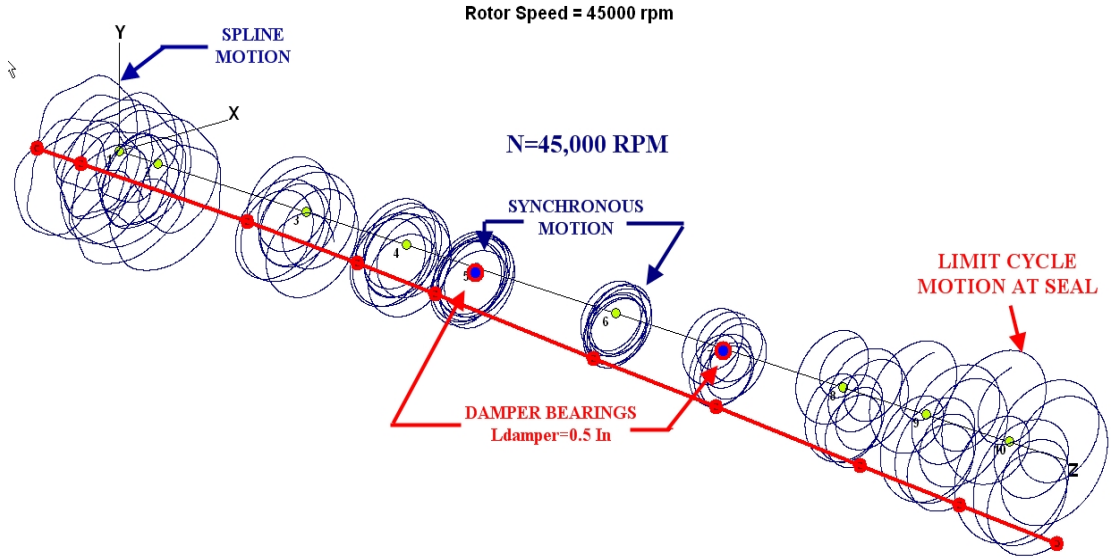

Fig. 25 Transient Motion At 45,000 RPM Showing Stable Limit Cycle Whirl Motion

Fig. 25 represents the transient motion at 45,000 RPM. The motion is stable limit cycle cylindrical whirl. The shaft centerline in now in a cylindrical mode shape as contrasted to the conical mode shape as shown in Fig. 23. Conical motion as shown in Fig. 23 is more apt to result in impeller rubs.

4.3 Synchronous Response With High 2 Plane Unbalance, Ub=0.5 OZ-In

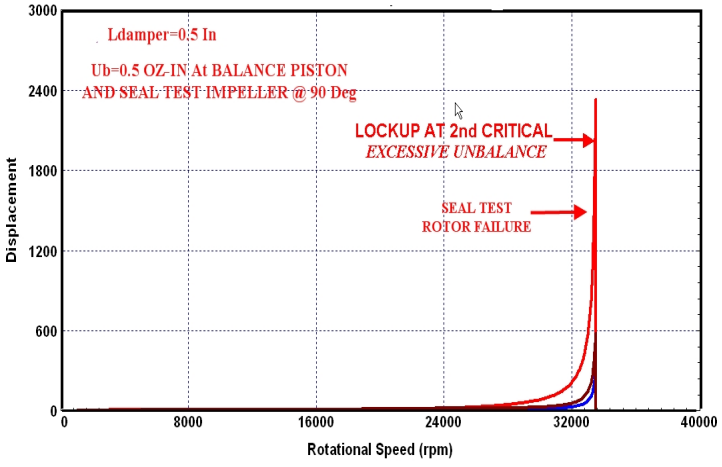

Fig. 26 Synchronous Response With High Unbalance

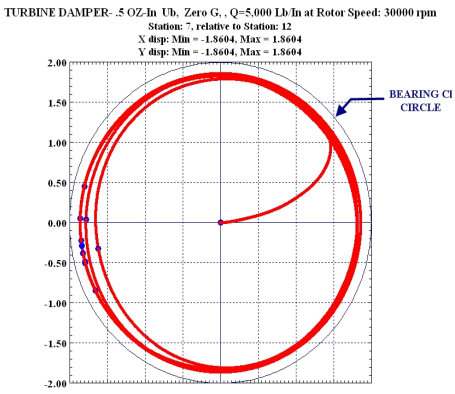

Fig. 27 Relative Damper Motion At 30,000 RPM Showing High Eccentricity

Fig. 26 represents the nonlinear unbalance synchronous response if the two planes of unbalance are increased from 0.1 to 0.5 oz-In. This causes the damper bearing to lock up resulting in a high 2nd critical speed response that would not be possible to operate through. Fig. 27 represents the time transient orbit at the seal test disk at 30,000 RPM with the large amount of unbalance. Superimposed on this orbit is the bearing damper clearance circle of 2 mils radius. The orbit is at 90% of the clearance circle. This condition is referred to as damper lockup. Thus we see that there are limits to the unbalance that can be applied to the rotor. This is not a problem if reasonable balance levels are maintained.

Damper Lockup Control By Damper Flexible Support

The damper lockup as seen in Fig. 26 is the result of the high unbalance causing the damper to orbit at 90% of the squeeze film damper bearing clearance. Under these circumstances, the radial oil film stiffness approaches the stiffness of the supporting rolling element bearing. This lockup condition may be controlled by the proper design of the damper supporting structure.

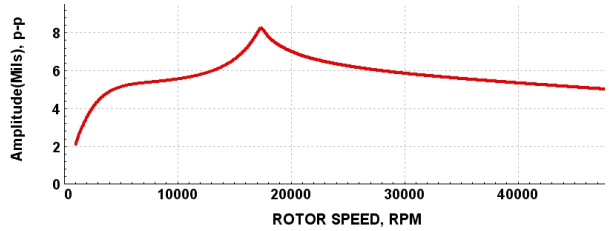

Fig 28 Disk Response With Reduced Foundation Stiffness

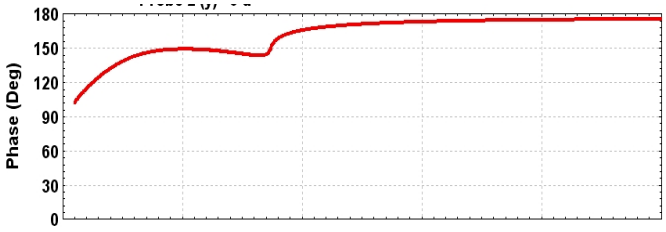

Fig 29 Disk Response Phase

Fig. 28 represents the nonlinear response of the test rotor with the high value of unbalance. The supporting structure of the damper, which was assumed to be rigid, has been placed by a flexible structure with a support stiffness of Ksup = 250,000 Lb/in. This is very typical with aircraft engine supports. By incorporating the flexible supporting structure with the squeeze film damper , the problem of damper lockup has been alleviated. The flexible support has made the system response more linear.

Fig. 29 shows the corresponding phase of motion for the disk. The flexible support has reduced the 2nd critical speed from around 30,000 RPM to 17,000 RPM. Although it is not feasible with the current test rig to incorporate a flexible damper support, it should be kept in mind that this is a technique that will allow one to minimize the damper lockup problem which is a serious problem with both center and non centered squeeze film dampers.

Fig. 30 represents the synchronous unbalance response mode shape at 17,350. This speed corresponds to the new rotor 2nd critical speed as seen by the cylindrical in phase mode shape of the motion.

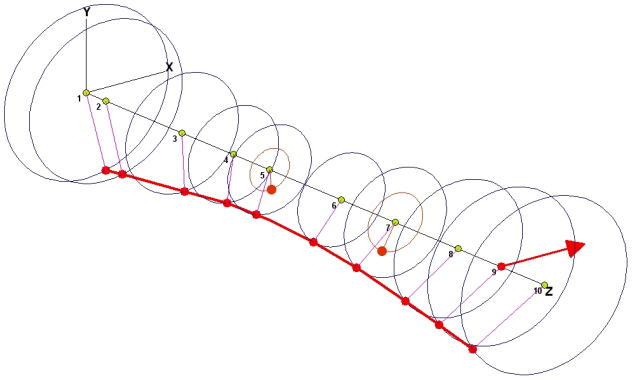

Fig. 30 Response With High Unbalance at 17,350 RPM With Flexible Damper Support

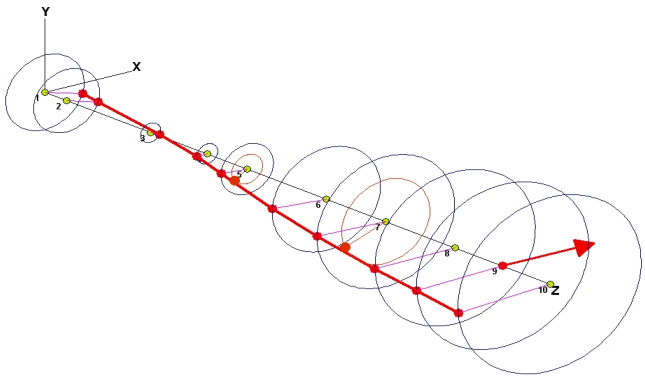

Fig. 31 Response With High Unbalance at 50,000 RPM With Flexible Damper Support

Fig. 31 represents the rotor motion at 50,000 RPM (which is above the design max speed of the rig). Note that the disk motion is out of phase from the disk unbalance. Thus the rotor motion remains relatively unchanged from a speed range of 30,000 to 50,000 RPM. In the actual NASA test rig, however, since the supporting structure is very rigid, the test rotor must be reasonably balanced to avoid lockup.

5. DISCUSSION AND CONCLUSIONS

In the design of high speed rotors mounted in rolling element bearings, it is necessary to provide some form of damped flexible support in order to pass through the critical speeds without bearing distress. In addition to the critical speed problem, damping at the bearings or support is also required to prevent self excited whirl motion caused by internal friction or Alford type of forces acting at impellers and balance pistons. A common type of damper employed with rolling element bearings is the squeeze film damper bearing. This bearing -damper configuration is very common in aircraft gas turbine engines. The damper may or may not have a centering spring. The centering spring is needed on heavily loaded rotors to support the gravitational loads. In the case of the seal test rig, the centering spring design was not used. The uncentered design used is similar to the design used in many aircraft LP and HP gas turbine rotors.

The design and analysis of this type of bearing is complicated by the nonlinear nature of the squeeze film damping characteristics. When the bearing is centered in the damper, the film stiffness is zero. As the bearing housing precesses in the damper clearance, the damper radial squeeze film stiffness increases rapidly. If the orbital motion in the damper exceeds 70% of the clearance, then damper lockup may occur. Even a well designed damper may experience damper lockup with excessive unbalance. It is shown that the nonlinear damper lockup problem may be eliminated by the incorporation of a properly designed flexible supporting structure. Computer simulation is required for proper design.

REFERENCES

1. Alford,J.S., ***Protecting Turbomachinery From Self-Excited Whirl***, ASME Jour. Of Engr. For Power, Vol 87, Oct., 1965, pp. 333-344
2. Barrett, L. E., and Gunter, E. J., ***Steady State and Transient Analysis of a Squeeze Film Damper Bearing for Rotor Stability***, NASA CR-2548, (1975).
3. Chen, W. J., and Gunter, E. J., ***DyRoBes Reference Manual on Rotor Bearing Dynamics, version 9***, RODYN Vibration Analysis, Inc., Charlottesville, VA, 22903 (2004).
4. Chen, W. J., and Gunter, E. J., ***Introduction to Dynamics of Rotor-Bearing Systems***, Trafford Publishing, Victoria, B.C., Canada, (2005).
5. Gunter, E. J., Barrett, L., E., Allaire, P. E., ***Design of Nonlinear Squeeze Film Dampers For Aircraft Engines***, ASME Journal of Lubrication, Vol. 92, No. 1 (1977) 57-64.
6. Kirk, R. G., and Gunter, E. J., ***Nonlinear Transient Analysis of Multi-Mass Flexible Rotors-Theory And Applications***, NASA CR-2300, Washington, DC (1973)
7. Proctor, M. P., Kumar, A., and Delgado, I. R., ***High-Speed, High-Temperature Finger Seal Test Results***, Journal of Propulsion and Power AIAA, Vol. 20, No. 2, (2004) 312-318.
8. Proctor, M. P., and Delgado, I. R., **Leakage and Power Loss Test Results for Competing Turbine Engine Seals**, NASA/TM-2004-213049, ARL-TR-3157, GT2004-53935, (2004).
9. Proctor, M. P., and Gunter, E. J., ***Nonlinear Whirl Response of a High-Speed Seal Test Rotor With Marginal and Extended Squeeze-Film Dampers***, NASA/TM-2005-213808, ISCORMA-3 Paper No. 212, Cleveland, OH, (2005).